



1 **Coupling biophysical processes and water rights to simulate spatially distributed**
2 **water use in an intensively managed hydrologic system**

3 **Bangshuai Han¹, Shawn Benner², John Bolte³, Kellie B. Vache³, Alejandro N. Flores²**

4 ¹ *Natural Resources and Environmental Management, Ball State University, Muncie, IN, 47306, USA*

5 ² *Geosciences, Boise State University, Boise, ID, 83725, USA*

6 ³ *Biological & Ecological Engineering, Oregon State University, Corvallis, OR, 97333, USA*

7 *Correspondence to: Alejandro N. Flores (LejoFlores@boisestate.edu)*

8 **Abstract:** Humans have significantly altered the redistribution of water in intensively managed
9 hydrologic systems, shifting the spatiotemporal patterns of surface water. Evaluating water
10 availability requires integration of hydrologic processes and associated human influences. In this
11 study, we summarize the development and evaluation of an extensible hydrologic model that
12 explicitly integrates water rights to spatially distribute irrigation waters in a semi-arid agricultural
13 region in the Western United States, using the Envision integrated modeling platform. The model
14 captures both human and biophysical systems, particularly the diversion of water from the Boise
15 River, which is the main water source that supports irrigated agriculture in this region. In
16 agricultural areas, water demand is estimated as a function of crop type and local environmental
17 conditions. Surface water to meet crop demand is diverted from the stream reaches, constrained
18 by the amount of water available in the stream, the water rights-appropriated amount and the
19 priority dates associated with particular places of use. Results, measured by flow rates at gaged
20 stream and canal locations within the study area, suggest that the impacts of irrigation activities
21 on the magnitude and timing of flows through this intensively managed system are well captured.
22 The multi-year averaged diverted water from the Boise River matches observations well, reflecting
23 the appropriation of water according to the water rights database. Because of the spatially explicit
24 implementation of surface water diversion. The model can help diagnose places and times that
25 water resources is likely insufficient to meet agricultural water demands, and inform future water
26 management decisions.

27 **Highlights:**

- 28
- 29 • A novel tool that explicitly integrates water rights to spatially allocate irrigation
 - 30 • Captures elements of both human and biophysical systems
 - Inform future water management policies and decisions

31 **Keywords:** Integrated modeling; Treasure Valley; Irrigation; HBV; Water use; Water right



33 1 Introduction

34 1.1 Background

35 Increasing water demands for both agricultural and domestic consumption under the stress of
36 climate change and increasing population represents a global environmental challenge
37 [Vörösmarty *et al.*, 2000]. This increasingly limited hydrologic supply exists within the context of
38 often extensive built hydrologic infrastructure. In turn, the management of that infrastructure is
39 driven by complex social processes and decision making [Pahl-Wostl, 2007]. Accordingly,
40 projecting how climate change and human activities will alter water availability in the future
41 requires developing models that can integrate human decision making and biophysical processes
42 [Girard *et al.*, 2015]. This challenge is particularly acute in arid and semi-arid regions where water
43 resources are typically limited and actively managed to support irrigation-supported agriculture
44 [Falkenmark, 2013].

45 Explicit integration of both human and environmental processes in hydrologic modeling is an area
46 of active investigation and a variety of approaches are being used. For example, *Jakeman and*
47 *Letcher* [2003] introduced attempts in Australia to integrate between hydrological and economic
48 models using a nodal network approach. *Ahrends et al.* [2008] developed a coupled model
49 system, consisting of a distributed hydrological model and an economic optimization model,
50 communicating via model interfaces, to investigate regional interdependencies between irrigated
51 agriculture and regional water balance in West Africa. *Ferguson and Maxwell* [2012] applied an
52 integrated hydrologic model to compare effects of climate change and water management on
53 terrestrial water and energy budgets of a representative agricultural watershed in the semi-arid
54 Southern Great Plains of the United States. *Willaarts et al.* [2012] discussed win-win management
55 solutions through societal evaluation of hydrological ecosystem services. *Cai et al.* [2013]
56 evaluated potential hydrologic alterations of the Yangtze River under four scenarios of reservoir
57 operation strategies by balancing human and environmental factors. *Kirby et al.* [2013] conducted
58 a basin-wide simulation of flows and diversions for economic and policy analysis in the Murray-
59 Darling Basin. *Laniak et al.* [2013] summarized recent progress and difficulties of integrated
60 environmental modeling and urged that global community of stakeholders transcend social, and
61 organizational boundaries and pursue greater levels of collaboration.

62 In the arid and semi-arid regions agriculture often relies heavily on irrigation and is typically the
63 largest water use [Döll and Siebert, 2002; Shiklomanov, 2000]. Irrigation diverts water to the



64 originally dry lands, significantly altering the hydrological cycle. Because amount and timing of
65 applied irrigation water is, ultimately, a local decision made by farmers for individual fields, it is
66 particularly challenging to explicitly express these changes in a way that captures resulting
67 spatially and temporally variable impacts.

68 A variety of approaches have been taken to express irrigation in hydrologic models. Many models
69 rely on a simple soil-water balance module, and empirically estimate the agricultural water
70 demand. For example, *Gisser and Mercado* [1972] applied empirically estimated agricultural
71 water demand into a hydrologic model in Pecos Basin. *Döll and Siebert* [2002] developed a global
72 irrigation model to calculate the irrigation water requirements depending actual and potential
73 evapotranspiration rates. *Cai et al.* [2012] applied an irrigation diagnosis model to a regional
74 irrigation system in the Yangtze River Basin to analyze the local water budget. These models are
75 advantageous for hydrologic-economic assessment, but typically discount some details of the
76 physical system. Physically based models can simulate processes influencing the water balance,
77 including crop growth, irrigation, fertilizer applications and solute transport. Examples include the
78 soil-water-atmosphere-plant (SWAP) model [*Dam et al.*, 1997; *Droogers et al.*, 2000], the
79 Environmental Policy Integrated Climate (EPIC) model [*Gassman et al.*, 2005] and the CropSyst
80 model [*Stöckle et al.*, 2003]. Generally, these models are operated as point-scale models and do
81 not express processes in a spatially explicit manner. With expanded computational capacity and
82 the progress of GIS, increasing interest has been put on the integration of agricultural based
83 models with spatially-distributed hydrologic models, e.g., VIC-CropSyst [*Stöckle et al.*, 2014],
84 GEPIC [*Liu et al.*, 2007]. Generally, the commonly used approach in irrigation modeling is to set
85 soil moisture to field capacity or soil saturation or set a fixed evapotranspiration rate in irrigated
86 areas [*Leng et al.*, 2014], which can lead to inaccurate water budget and an inability to represent
87 irrigation in a more realistic way. It is also a common practice to assume unlimited water supply
88 when considering the sources and availability of irrigation water, which does not reflect the truth
89 in many water limited environments [*Sorooshian et al.*, 2012]. As such, we are aiming to
90 incorporate irrigation activities in our model in a more realistic way.

91 In the western United States, water is mostly allocated according to legally defined water rights
92 following the Prior Appropriation Doctrine, which basically defines that water rights are determined
93 by priority of beneficial use; historical use of water creates a right to the water. This means that
94 the irrigation amount is dependent not only on physically defined water availability, but also on
95 constraints dictated by legally defined water rights. In these systems water use for irrigation is,
96 therefore, the product of both environmental constraints (e.g. basin scale water availability and



97 evaporative demand) and human constraints through water rights allocations. Accordingly, water
98 rights represent an important, and well defined, constraint on irrigation water use in these
99 systems. However, few models take consideration of the influence of water rights on the
100 redistribution of water. The state of Texas has implemented a modeling system called Water
101 Rights Analysis Package (WRAP) to assess water availability and reliability of water resources
102 with local water rights [Wurbs, 2005a; b], but the model is not fully spatially distributed and the
103 model functions on a monthly scale.

104 In this study, we demonstrate an approach that integrates water diversion for irrigation based on
105 water rights within a physically-based model of hydrologic processes. We outline the development
106 of the core elements of both the biophysical and social system components of the model that
107 appear critical to represent the redistribution of water within the study area.

108 1.2 Study area

109 The Treasure Valley area, located in southwest Idaho, is the most populous region of Idaho and
110 contains its three largest cities, Boise, Nampa and Meridian (Figure 1), but is also home to an
111 extensive irrigation-supported agriculture. The area collectively comprises about 40% of state's
112 total population, with an area of 3323 km². Farm land occupies about 40% of the total
113 landscape, with an area of 1289 km², and relies heavily on irrigation through about 1700 km of
114 constructed canals.

115 Climate is generally semi-arid Mediterranean pattern with a hot dry summer and cold wet winter,
116 with strong spatial and temporal fluctuations in temperature and rainfall. Annual rainfall varies
117 substantially within the basin from ~ 700 mm in the northeast foothills to ~ 200 mm in the
118 southwest at the Lake Lowell, with a historical average of about 296 mm/yr at Boise Air
119 Terminal weather station. About 50% of the total precipitation occurs during the non-irrigation
120 season. Like many intensively managed landscapes in semiarid and mountainous regions of the
121 world, a series of reservoirs upstream of the Treasure Valley regulate and homogenize flows out
122 of the upper basin into the Boise River. The lower-most of these reservoirs, Lucky Peak, is
123 operated jointly by the US Army Corps of Engineers and the Bureau of Reclamation for
124 purposes of flood control and irrigation water supply. From Lucky Peak Reservoir, the Boise
125 River exits the mountains and flows about 103 km (64 miles) northwestward through the
126 Treasure Valley to its confluence with the Snake River. The Treasure Valley is bounded to the
127 north by the Boise foothills and to the south by the Snake River. A number of canals and
128 diversion dams have been built along the Boise River water course to allocate water resources.



129 Among the largest of these canals is the New York Canal that diverts water directly from the
130 Boise River about 1.6 km downstream of the Lucky Peak dam. During non-irrigation season, the
131 New York Canal carries a portion of the water to fill Lake Lowell, a reservoir within the Treasure
132 Valley area, for use during the irrigation season. During irrigation season, the New York Canal
133 carries a significant portion of the water from the Boise River and diverts it into distributary
134 canals within the agricultural areas of the Treasure Valley. With the benefit of irrigation,
135 population in the Treasure Valley has been growing rapidly and consistently since the 1870s.
136 Urban growth and increasing irrigation activities drive land use change and reallocation of water
137 resources. Despite the importance of water resources and potential threats of water scarcity,
138 there have been limited integrative studies regarding water availability and scarcity in this area.
139 The Idaho Department of Water Resources (IDWR) conducted the Treasure Valley Hydrologic
140 Project starting in 1996, aiming to develop a better understanding of water resources in the
141 Treasure Valley and to evaluate changes in regional and local groundwater conditions.
142 Supported by this project, *Petrich [2004b]* characterized and simulated groundwater flow in the
143 Lower Boise River Basin, and analyzed the water budgets for the regional aquifer system based
144 on 1996 and 2000 calendar-year inflow and outflow estimates [*Petrich, 2004b; Urban and*
145 *Petrich, 1996*]. Local, state, cities and some federal agencies have also supported or conducted
146 a few water demand studies that characterized the local land use and the associated domestic,
147 commercial, municipal, and industrial water demands. However, most of these studies are
148 conducted at the conceptual level by estimating total water budgets. *Xu et al. [2014]* conducted
149 a hedonic analysis to estimate the response of agricultural land use to water supply information
150 under the Prior Appropriation Doctrine. Their results are informative at the scale of the entire
151 Treasure Valley but also lack spatiotemporally dynamic components that could be used to
152 reveal particular locations in space and periods in time where water demand and supply are out
153 of balance. This research seeks a practical integration of the spatiotemporal detail that is
154 available in the water rights database with the local spatiotemporal dynamics of surface water
155 hydrology. An important outcome of this study is an extensible modeling framework that can
156 serve as a foundational tool to capture and evaluate the complex interactions between the
157 social and biophysical systems related to water use in an integrated way.

158

159

160

Figure 1 Study Area: the Treasure Valley.

161 2 Methods



162 2.1 Envision platform and datasets

163 The model developed in this study is based on the Envision modeling tool, a spatially explicit
164 integrated simulation platform that can be used to integrate elements of biophysical and social
165 systems [J P Bolte *et al.*, 2007; Inouye, 2014]. Envision provides a geospatial software
166 framework to coordinate the interoperation of component models used to represent essential
167 processes and properties of the coupled social and biophysical systems being simulated.
168 Envision has been used in a variety of projects, e.g., to develop alternative future scenarios
169 under three growth management strategies for the Puget Sound Region in Washington, US [J
170 Bolte and Vache, 2010], construct a land use / land cover (LULC) agent based modeling for the
171 Motueka catchment, Australia [Montes de Oca Munguia *et al.*], evaluate potential impacts of
172 climate change on vegetation cover in the Willametter River Basin, Oregon, US [Turner *et al.*,
173 2015], and understand coupled natural and human systems on fire prone landscapes [Barros *et al.*,
174 2015].

175 In Envision, the spatial domain is represented by a collection of polygons, called Integrated
176 Decision Units (IDUs). Each IDU polygon is associated to important geospatial attributes
177 characterizing both biophysical and social properties (e.g., elevation, soil type, land use,
178 population density, disturbance history, water right code, irrigation decision etc.). The IDU forms
179 the fundamental spatial unit for integrated decision-making in Envision. The process of creating
180 the IDU computational domain is somewhat ad hoc and iterative, but is meant to balance the
181 competing demands of fidelity to spatial heterogeneity and associated computational cost. The
182 IDU computational domain was constructed through a process that initially converted raster-
183 based LULC information into a polygon layer by grouping adjacent sets of pixels with similar
184 land-use/land-cover classes into polygons. Small polygons derived from a single LULC pixel
185 within a larger polygon of a different land-use/land-cover class (i.e., with an area of 900 m² or
186 less) were identified and deleted. The final constructed computational domain for the Treasure
187 Valley consists of 32,508 IDUs (polygons).

188 A variety of dataset is required to build the model (Table 1), among which, spatial heterogeneity
189 in the model is mainly reflected by three spatially explicit datasets: land cover, elevation, and
190 meteorological inputs. The land cover data is collected from the Nation Land Cover Dataset,
191 using the data of 2011. The elevation data is collected from the National Elevation Dataset with
192 a spatial resolution of 30 m. The climate dataset is a spatially and temporally complete, high-
193 resolution (4-km) gridded dataset of surface meteorological variables created by bias-correcting
194 daily and sub-daily mesoscale reanalysis and assimilated precipitation from the NLDAS-2 using



195 monthly temperature, precipitation and humidity from Parameter-elevation Regressions on
196 Independent Slopes Model [*Abatzoglou and Brown, 2012*]. The stream network is defined from
197 the NHDPlus V2 dataset, which represents stream networks as node-based line coverages.
198 Segments between nodes are considered to be stream reaches and each IDU is assigned a
199 stream reach for the purposes of simulating hydrologic routing. Artificial channels such as
200 irrigation canals and drains are explicitly represented. However, as discussed below, they are
201 functionally captured using the WaterMaster module, which simulates the allocated water based
202 on water rights.

203

204 Table 1 Datasets used in the model

205

206 2.2 Hydrologic processes

207 In this study, we employ the module called Flow with a slightly changed Hydrologiska Byråns
208 Vattenbalansavdelning (HBV) [*Bergström and Singh, 1995; Woodsmith Richard D. et al., 2007*]
209 plugin to represent hydrologic processes. Human interventions include reservoir operations, and
210 agricultural irrigation which is simulated by another Flow plugin called WaterMaster. The primary
211 focus of the current paper is to develop a framework to incorporate human activities, mainly
212 irrigation, at the watershed scale, and provide solid basis for future integrated scenario
213 projections.

214 Within Envision, the HBV model is applied in a semi-distributed way to delineated Hydrologic
215 Response Units (HRUs) within the study domain affording the use of spatially distributed
216 datasets such as daily gridded meteorological inputs, land cover, and elevation information
217 [*Inouye, 2014*]. Within the model, HRUs are delineated by aggregating adjacent IDUs that are
218 associated with a common LULC and similar elevation, and 4456 HRUs are composed.
219 Hydrologic processes are simulated at the HRU-level, with fluxes being distributed uniformly to
220 the IDUs within the HRU.

221 Here, we briefly describe the slightly changed HBV model (Figure 2). A catchment in the model
222 is conceptualized as a series of linked reservoirs and is divided into 6 layers in this study:
223 snowpack, melt, irrigated soil, non-irrigated soil, upper groundwater and lower groundwater.
224 Runoff from the HRUs from different layers is then routed to streams using linear outflow
225 equations. The water balance equation in Flow (HBV) can be described as:



226
$$P - ET - Q = \frac{d}{dt}[SP + SM + UZ + LZ + lakes]$$
 Eq. 1

227 where, P = precipitation; ET = evapotranspiration; Q = runoff; SP = snow storage; SM = soil moisture
228 storage; UZ = upper groundwater storage; LZ = lower groundwater storage; $lakes$ = lake storage.

229 The model simulates daily discharge using daily rainfall, temperature, and potential
230 evapotranspiration as inputs. Precipitation is simulated to be either snow or rain depending on
231 whether the temperature is above or below a threshold temperature (TT). Rainfall and snowmelt
232 are then divided into water either filling the conceptual soil layer or recharge into groundwater
233 depending on the current soil moisture, field capacity (FC), and the parameter “Beta” (Eq. 2).

234
$$F = \left(\frac{\text{Soil Water}}{FC}\right)^\beta$$
 Eq. 2

235 where, F is the fraction of rain or snow. Evapotranspiration (ET) is simulated using the FAO56
236 Penman-Monteith method as specified by the UN Food and Agriculture Organization (FAO) in
237 paper number 56 [Allen *et al.*, 1998] and in [Allen and Robison, 2007]. Generally, a crop
238 coefficient K_c is developed to simplify and standardize the calculation and estimation of crop
239 water use, and is an integration of the effects of crop properties and soil properties. As plants
240 grow and develop, K_c varies over time and the values are obtained from AgriMet Pacific
241 Northwest Cooperative Agricultural Weather Network. The potential ET of a specific crop, ET_c , is
242 then calculated as in Eq. 3:

243
$$ET_c = K_c * ET_r$$
 Eq. 3

244 where, ET_r is the reference evapotranspiration rate, the evapotranspiration rate for a
245 standardized vegetated surface corresponding to a living, agricultural crop (usually using full
246 cover alfalfa). For simplicity at this framework building stage, we do not include detailed crop
247 categories and crop rotation schedules. Rather, we use the crop coefficients of alfalfa for all
248 agricultural land use in the region due to the fact that most of the agricultural land in the
249 Treasure Valley is fully irrigated. Crop coefficients are assigned for non-agricultural lands based
250 on crop categories with a similar physical characteristics as an approximation (Table 2).
251 Detailed evapotranspiration calculation methods could be referred to [Allen and Robison, 2007].
252 Actual ET in the model is constrained by soil moisture at each HRU, as simulated in each daily
253 time step. The soil box is subdivided into two layers/fractions, irrigated soil and non-irrigated



254 soil, to help facilitate water to be irrigated and evaporated from the irrigation areas. The
255 response function consisting of two or three linear outflow equations depending on whether or
256 not recharge in the upper groundwater box (SUZ) is above a threshold value (UZL) then
257 transforms excess water from the soil layer to runoff (Eq. 4, Eq. 5, and Eq. 6).

$$258 \qquad \qquad \qquad Q_0 = K_0 \cdot (SUZ - UZL) \qquad \qquad \qquad \text{Eq. 4}$$

$$259 \qquad \qquad \qquad Q_1 = K_1 \cdot SUZ \qquad \qquad \qquad \text{Eq. 5}$$

$$260 \qquad \qquad \qquad Q_2 = K_2 \cdot SLZ \qquad \qquad \qquad \text{Eq. 6}$$

261 where, SUZ is the recharge (water depth) at the upper groundwater zone that is simulated at
262 each time step, UZL is a threshold value, SLZ is the recharge (water depth) at the lower
263 groundwater zone that is simulated at each time step. If $SUZ \geq UZL$, then the total water that
264 is routed to runoff is the summation of Q_0 , Q_1 and Q_2 . If $SUZ < UZL$, then the total water that is
265 routed to runoff is the summation of Q_1 and Q_2 .

266 Table 2 Crop categories used to approximate the land use categories in the ET calculation

267 Figure 2 Flowchart of the Flow module in Envision. Note the human activities influencing water
268 availability. Water is distributed by the local water rights data (irrigation activities), and is also
269 constrained by the reservoir operations.

270 2.3 Simulation of water rights

271 Irrigated water allocation is simulated via a module called Watermaster (Figure 3) that adheres
272 to publicly available water rights data in Idaho in accordance with the Prior Appropriation
273 Doctrine [Hutchins, 1977; Xu et al., 2014]. In this study, surface water and groundwater
274 irrigation activities are simulated based on the water rights data updated in 2012 by IDWR. Each
275 water right is associated with four attributes that are of critical importance to this study: (1) the
276 Place of Use (POU), (2) the Point of Diversion (POD), (3) the priority date, and (4) the
277 appropriated diversion rate.

278 The POU data is used to identify IDUs in the study domain with surface water and/or ground
279 water rights. For surface water rights, water is extracted from the stream reach closest to the
280 POD associated with that water right. In most cases in the Treasure Valley, the PODs are
281 located along irrigation canals not explicitly being simulated, and the PODs are assumed to be



282 the point at which water is originally diverted from a natural watercourse (A majority originally
283 diverted from the Boise River due to its seniority and largest diversion capacity) into the
284 associated supply canal system. The priority date of each water right determines whether or not
285 water can be diverted from the stream reach associated with the POD and applied to the IDUs
286 within a POU as irrigation on a particular date during the simulation. On each day of the
287 simulation, WaterMaster determines all water rights active on that date and, based on the
288 allocation rates of those water rights, determines the maximum flow of water that may be
289 diverted at each stream reach associated with one or more PODs. The irrigation water demand
290 at the POU is computed as the potential evapotranspiration for the agricultural IDUs within each
291 POU with a composite loss coefficient which is currently set based on an overall estimation of
292 60% water loss from the original diversion to ultimate crop use. The coefficient was roughly
293 estimated based on a local study of irrigation management in 1999 and the proposed potential
294 improvement in the study to reflect the current irrigation efficiency [Huter *et al.*, 1999]. The
295 amount of water demanded for diversion at the stream reach is then computed as the sum of
296 water demand for all POUs associated with a POD along that reach. If there is sufficient
297 streamflow to satisfy demand, the amount of water diverted equals the total demand. If there is
298 insufficient streamflow in the reach to satisfy demand, then water rights must be curtailed. Water
299 rights with highest seniority (i.e., earliest priority date) are satisfied and streamflow reduced by
300 the allocation rate associated with that right, followed by the next most senior water right, and so
301 forth until there is insufficient streamflow to meet demands of water right. At this point, that
302 water right and all more junior rights are curtailed only for the current date and will resume water
303 use whenever there is abundant stream flow later of the year. This approach simulates the
304 effect of canals and distributaries without explicitly simulating the hydraulics of canal flow.
305 Specifically, water is diverted from an actual place of diversion as captured by the IDWR
306 database and applied to a place of use in accordance with the water rights database. For
307 ground water rights, we assume unlimited groundwater source as of now due to the fact that
308 groundwater resources are abundant for the withdrawal rates in the Treasure Valley [Petrich,
309 2004a]. On the valley-wide basis, the volume of ground water pumped during the year accounts
310 only 15 to 20% of the total ground water recharge [Urban and Petrich, 1996]. Groundwater in
311 the Treasure Valley is mainly recharged from the seepages from the canal system, flood
312 irrigation and precipitation. Use of groundwater for irrigation is common, although surface water
313 rights comprise a much larger proportion of agricultural water use on a volume basis in the
314 Treasure Valley.

315 Here we would like to define a couple important terms used below:



316 The allocated water indicates the amount of water that is met and diverted to the corresponding
317 place of use in the model.

318 The unsatisfied water indicates the amount of water that is not met for the corresponding place
319 of use in the model.

320 The appropriated diversion rate is calculated based only on the POD rates and the
321 corresponding POUs, and reflects the amount of water that is potentially usable based on the
322 existing water right maximum rates while ignores priority dates and physical constraints. It is
323 calculated upon the water right dataset instead of being simulated by the model.

324

325 Figure 3 WaterMaster loop that makes use of the local water rights data for irrigation

326 2.4 Reservoirs and boundary condition

327 Reservoirs are considered part of the stream network in Envision. The location and physical
328 constraints of the Lucky Peak Reservoir and Lake Lowell's dams are set up based on the data
329 collected from the Hydromet database (Table 1). The Lucky Peak Reservoir receives water
330 drained from the watersheds upstream of Boise River, and is the main water resources for the
331 Treasure Valley. The historical inflows to the Lucky Peak Reservoir are used as inflow boundary
332 condition for the model. Lake Lowell is an offstream reservoir formed by three earthfill dams
333 enclosing a natural depression at southwest Treasure Valley. The reservoir naturally drains
334 water and is also filled during the non-irrigation season by diversions at the Boise River
335 Diversion Dam through New York Canal. In this study, we simplify the reservoir operations by
336 setting the maximum and minimum flows at a downstream control point of each reservoir (Boise
337 River at Diversion Dam for Lucky Peak Reservoir and Boise River near Parma River for Lake
338 Lowell) based on historical daily extreme values to regulate the extreme flow released from the
339 reservoirs. This setup is efficient while still simulates the normal operation of the Boise Project
340 Board of Control. The operation basically aims to control flood in the Boise River for the safety
341 of the city, uses the natural river flows until the Boise River falls to a certain level, and then
342 switches to water stored in reservoirs and provides users a certain allotment of water they can
343 use for the irrigation season. As such, by setting up maximum and minimum daily flows, the
344 reservoirs are designed to release water in the dry seasons and control flooding water in the
345 snow melt season of the area.

346 2.5 Model calibration and validation methods



347 The reliability of many hydrological models is dependent on calibration, which is the process of
 348 finding an optimal set of parameters that enable the model to closely match the behavior of the
 349 real system it represents [Gupta *et al.*, 1998]. We calibrated the model based on the Nash-Sutcliffe
 350 coefficient (Eq. 7) between the observed and simulated stream flows at two USGS gages – Boise
 351 River at Glenwood and Boise River near Parma, Idaho.

352 The Nash-Sutcliffe coefficient is calculated as:

$$353 \quad E = 1 - \frac{\sum_{t=1}^T (Q_{obs}^t - Q_{sim}^t)^2}{\sum_{t=1}^T (Q_{obs}^t - \overline{Q_{obs}})^2} \quad \text{Eq. 7}$$

354 where, Q_{obs} is the observed discharge; Q_{sim} is the simulated discharge, and t is the time step at
 355 calculation, $\overline{Q_{obs}}$ is the mean observed discharge over the entire run. Nash-Sutcliffe efficiencies
 356 can range from $-\infty$ to 1 (perfect match). An efficiency of negative value indicates that the mean
 357 value of the historical observations would be a better predictor than the hydrologic model.
 358 Most parameters used in the model are estimated using a Monte Carlo approach. The data from
 359 years of 2006 - 2009 are used for calibration processes, and from 2010 - 2013 are used for
 360 validation purpose. For each run, each parameter value was randomly selected from a uniform
 361 distribution; the minimum and maximum values of these distributions, listed in table 3, are
 362 generally adopted from Sælthun [1996], Lawrence *et al.* [Lawrence *et al.*, 2009] and Abebe *et al.*
 363 [Abebe *et al.*, 2010]. We simultaneously vary the values of the parameters within their target
 364 ranges, and run the model 1000 times. Then the best-fit parameter sets are selected through an
 365 assessment of the fit of simulated to observed runoff data based on visual inspection of fit and
 366 Nash-Sutcliffe Efficiency (E) between the observed discharge and the simulated discharge. The
 367 parameters are conceptually based on physical parameters of the system. Although they are
 368 actually effective parameters that fit the model through calibration and do not necessarily
 369 represent actual physical properties, it would be beneficial to get physically representative
 370 values whenever possible. In this calibration process, we calibrate 9 parameters of the total
 371 14 parameters, while setting 5 parameters constant to save computational time. The FC and
 372 WP values were adopted from the SSURGO dataset from the Natural Resources Conservation
 373 Service. Since LP, CFR and CWH are not sensitive to model performance [Seibert, 1997], a
 374 reasonable LP value was set based on local soil conditions, and CFR and CWH were held
 375 constant.

376 Table 3 Parameters used, the range considered for calibration and the calibrated values

377



378 3 Results

379 In this section, the calibration and validation results of the hydrological module are presented, the
380 water right dataset is summarized, and the irrigation water use and water scarcity from 2006 –
381 2013 are analyzed.

382 3.1 Calibration and validation

383 The model was calibrated and validated against historical observations through discharge at two
384 USGS gaging stations (Boise River at Glenwood and Boise River near Parma) and at the New
385 York Canal. These two calibration targets reflect influences of different processes. The upper
386 gaging station (Glenwood) is just down-stream from the New York Canal, the primary point of
387 extraction but is up-stream of the majority of return flow to the Boise River, which is primarily in
388 the lower portion of the river. In contrast, the Parma gaging station is located just above the
389 confluence with the Snake River and is downstream of both the majority of the extraction and
390 return flows. Accordingly, model results that successfully match the Glenwood gage provide a
391 good indication of the model's capacity to simulate water consumption and associated removal,
392 while comparing the model results to the Parma gage is more strongly influenced by the model's
393 capacity to capture return flow.

394 A plot of the simulated and the observed flows at these two USGS sites for the calibration
395 period (2006 – 2009) and the validation period (2010 – 2013) is shown in Figure 4. The model
396 effectively captures the major high and low flow events, the extreme values of which are
397 constrained by the downstream control points. For example, at Glenwood, the annual discharge
398 is clearly dominated by three periods associated with late winter or spring high flows, irrigation
399 season flows, and fall-winter low flows. The NS coefficient, which is a criterion to estimate the
400 goodness of fit between observational data and simulated data, is 0.82 during the calibration
401 period and 0.67 during the validation period at the Glenwood site, and 0.69 during the
402 calibration period and 0.62 during the validation period at the Parma site. The good fit to the
403 Parma gage suggests the model captures return flow particularly well. We also compare the
404 amount of water diverted to the New York Canal with the simulated results, and find a good
405 match with a correlation coefficient of 0.92 (Figure 5), indicating that the model does a good job
406 of capturing the diversion amount from the Boise River.

407



408 Figure 4 Simulated discharge and the observations during the calibration (2006 ~ 2009) and
409 validation periods (2010 ~ 2013) at the Glenwood Station of Boise River (Upper Panel) and
410 Parma Station of Boise River (Lower Panel).

411

412 Figure 5 Simulated irrigation amount and the observations averaged over the years of 2006 ~
413 2013 at the New York Canal. Blue color lines are daily discharge rate in m^3/s , and red color
414 lines are cumulative discharge in m^3 .

415

416 3.2 A summary of the irrigation water rights

417 In the Treasure Valley, surface water is the main water source for irrigation, despite many more
418 POD's for groundwater. Currently, there are 22,217 PODs and 21,492 places of use (POUs) in
419 the study area, among which, 4,838 PODs and 3,859 POUs are appropriated for the irrigation use
420 (Figure 6). In the following analysis, all water rights are irrigation water rights unless stated
421 otherwise. Within all water rights database, 78% of the PODs use groundwater as water source,
422 and only 22% use surface water as water source. However, surface water is still the main water
423 source with regard to the amount of irrigated water supply. Surface water PODs are mainly located
424 along the Boise River, usually with a relatively higher maximum allowed diversion rate per POD
425 (maximum $38.21 \text{ m}^3/\text{s}$), while groundwater PODs are dispersed all over the irrigated lands,
426 usually with a relatively smaller maximum allowed diversion rate per POD (maximum $2.47 \text{ m}^3/\text{s}$).
427 Among all the surface water PODs, most surface water is mainly diverted from the Diversion Dam
428 which connects New York Canal with Boise River. Multiple PODs overlap at the Diversion Dam
429 with highly senior water rights, diverting about half of the stream flow from main branch of Boise
430 River during the irrigation season. The diverted water provides the water resources for Lake
431 Lowell and numerous irrigation canals downstream.

432 Figure 6 The spatial distribution of the Points of Diversion (PODs) for irrigation purpose, and the
433 maximum allowed diversion rates.

434 3.3 Model simulated spatial and temporal distribution of water use

435 Comparing simulated water use with that predicted based on appropriated rates suggests the
436 model does a good job of spatially distributing water use. The summarized appropriation rate
437 generally matches the boundary of the irrigation districts (Figure 7). According to the appropriation



438 rate, most of the water should be appropriated to the southwest part of the Treasure Valley, e.g.
439 Nampa-Meridian, and New York irrigation districts. In contrast, a relatively small amount of water
440 should be appropriated to those areas along the Boise River and into the Black Canyon irrigation
441 district which is located at the northwest part of the Treasure Valley.

442 Figure 7 The annual appropriated diversion rates calculated based on water rights maximum
443 allowed diversion rates and place of use, indicating the potential usable water. The irrigation
444 district boundaries and the names of major irrigation districts are also shown.

445 The model simulated allocation rate follows these spatial patterns of the appropriated rate (Figure
446 8). The southwest part of the study domain receives the most allocated water, while the northwest
447 part and the downstream section of Boise River is allocated less water (Figure 8).

448 Figure 8 The spatial distribution of the annual allocated irrigation water averaged over the
449 simulation period. The domain that is circled is Black Canyon Irrigation District, which receives
450 additional irrigation water from outside of the domain, where the water allocation is
451 underestimated.

452 The simulated water allocation confirms that surface water is the main water source with regard
453 to the amount of allocated water, as shown by the model simulated annual and monthly allocated
454 surface water rates, and allocated groundwater rates (Figure 9, Figure 10). The allocated surface
455 water discharge rate is $\sim 21.3 \text{ m}^3/\text{s}$ averaged over 2006 to 2013, while the allocated groundwater
456 is only $\sim 4.0 \text{ m}^3/\text{s}$.

457 Figure 9: Average daily allocated surface water, groundwater and unsatisfied surface water use
458 for each year.

459
460 Figure 10: Average daily allocated surface water, groundwater and unsatisfied surface water use
461 for each month from 2006 to 2013.

462 The simulated water allocation also reflects the seasonal irrigation water use pattern. The
463 irrigation season in the Treasure Valley occurs from April to November when precipitation is rare
464 and temperature is high. As expected, most of the irrigation activities happens from May to
465 October, representing over 95.6% of the annual total irrigation amount. The peak irrigation season
466 is June, July and August, which irrigates 61.1% of the annual irrigation amount.

467 4 Discussions

468 4.1 The model's contribution to inform decision-making



469 4.1.1 The model reveals water scarcity and its causes by unsatisfied water distribution

470 The irrigation water scarcity is divided into 4 categories based on the annual unsatisfied irrigation
471 water amount: Adequate Water Rights (< 100 mm deficit), Light Scarcity (100 – 300 mm deficit),
472 Medium Scarcity (300 mm – 600 mm deficit), and Heavy Scarcity (> 600 mm deficit). There is
473 less allocated water along the downstream section of Boise River, which also leads to higher
474 water scarcity in the area (Figure 11). The northwest part of the study area experiences light to
475 middle level water scarcity. Water scarcity is overall not serious in the Treasure Valley, however,
476 could pose a problem in the relatively dry years such as 2007, 2008 and 2013.

477 Figure 11: The spatial distribution of the annual unsatisfied irrigation maps averaged over the
478 simulation period. The domain that is circled is Black Canyon Irrigation District, which receives
479 additional irrigation water from outside of the domain, where the water scarcity is overestimated.

480 On average, ~ 80.1% irrigation demand could be satisfied from 2006 to 2013, with an unsatisfied
481 irrigation rate about 5.1 m³/s for the whole irrigation area. However, the unsatisfied irrigation
482 amount varies greatly between years. For example, in 2011 when the annual precipitation is
483 higher than normal (Figure 12), only an annual average of 3.4 m³/s irrigation amount is
484 unsatisfied in the Treasure Valley, while in 2013 when the annual precipitation is lower than
485 normal, the annual averaged unsatisfied irrigation amount doubled to about 5.9 m³/s (Figure 9).
486 The Mediterranean climate pattern produces dry-hot summers which, even in the wettest years,
487 some degree of unmet water potential irrigation use.

488 Figure 12 Annual precipitation amount calculated at Boise Air Terminal (Station ID:
489 7268104131). Precipitation is calculated based on water year since irrigation in each calendar
490 year is mainly affected by the precipitation during the spring and last winter.

491 While the water rights appropriation rate reflects the irrigation district regulation, the allocated rate
492 also considers the biophysical demand, and has the capacity to reveal where the current water
493 rights are not sufficient for biophysical use. For example, the areas along downstream Boise River
494 experience a relatively higher water scarcity (Figure 11). Since the Boise River has abundant
495 water to extract during the irrigation season as shown in the discharge figures (Figure 4), the
496 water scarcity is mainly due to the water right constraints. While this area is ascribed to be
497 agricultural land, the area is mainly used for grass/pasture (Figure 13), which does not require
498 much irrigation. Should these areas be converted to irrigated agricultural lands, they will need a



499 larger water right allocation to support crops. This illustrates the value of spatially explicit demand-
500 based water allocation and associated patterns to understand the irrigation water use dynamics.

501 Figure 13 The spatial distribution of crops and grass/pasture in the agricultural area of the
502 Treasure Valley.

503

504 4.1.2 The model indicates irrigation inefficiency through the simulation of demand-based water
505 allocation and the actual water use

506 Demand-based water allocation rates and the actual water use vary significantly. The allocated
507 water in an IDU is determined by the IDU water demand, the water availability in the stream and
508 water rights allocation rate and priority. The IDU water demand is calculated for irrigated lands
509 based on the potential ET rates and the water loss coefficient. However, the actual water use by
510 the farmers is usually more arbitrary relying on their experience, their irrigation methods and the
511 economic expectations, and is a complex function. Application efficiencies for traditional furrow-
512 irrigated systems supplied by siphon tubes or gated pipe range between 30 - 40%, with
513 efficiencies of 50 - 60% percent possible with excellent management [Neibling, 1997]. A large
514 amount of water is wasted even in this water-limited environment. The simulated multi-year
515 average of allocated surface water is ~ 2.0 acre-feet per acre. This number is in the lower range
516 of the allotted irrigation water by the Boise Project Board of Control which is about 2 – 3 acre-
517 feet per acre in normal years for farmer use. This can also be validated by the diverted amount
518 of water from the New York Canal (Figure 5), with an overall slightly underestimation but very
519 good match between simulations and observations (correlation coefficient of 0.92). Considering
520 that the water release at the operational level normally relaxes the biophysical demands and
521 varies annually, our simulated irrigation water amount is in the right scale.

522 4.2 Model Limitations

523 While the model appears to be an effective tool to express spatially explicit water rights based
524 allocation, there are some important features not captured by the model. Specifically, during the
525 dry years, e.g., 2007 and 2013, the model produces higher simulated discharge compared to the
526 observations at the Parma River gage during the irrigation season. There are a number of reasons
527 for these deviations in the model: (1) Groundwater use is currently assumed to be unlimited,
528 leading to extra amount of water recharged into soil layer. Although this reflects the current



529 groundwater abundance of the study area, it does not maintain the water balance after
530 groundwater irrigation, and may lead to larger simulated stream discharge at the downstream of
531 the irrigation area. However, since groundwater irrigation counts for a very small portion of the
532 irrigation water use, we intend to simplify the model at this stage by assuming an unlimited
533 groundwater supply. (2) The diversion of water in many canals are actually operated as constant
534 flows, differing from the demand-need diversion rates of the model. As such, it is implausible to
535 find a perfect match between observations and simulations. (3) The model is limited to the Boise
536 River watershed and only water within that watershed is considered. However, there is some
537 transfer into the basin from the adjacent watershed. This is especially important for the northwest
538 part of the Treasure Valley (mainly Black Canyon Irrigation District) where the model predicts
539 water scarcity (Figure 11). In reality, some water is pumped from Payette River outside of the
540 boundary to irrigate this area so it is very likely that the model is underestimating the water
541 allocation and exaggerating the water scarcity in this area. (4) The model is semi-conceptual, and
542 ignores some minor consumptive water use. For example, the water that is incorporated into
543 products or crops, consumed by humans or livestock, or otherwise removed from the immediate
544 water environment.

545 A second area where the model underperforms is capturing some flow details at the beginning of
546 each year. Local agencies tend to empty the reservoirs in the winter time for spring flood
547 protection, while the model ignores this local human operation. In addition, irrigation water use is
548 not only affected by weather conditions and irrigation at the current time step, but also affected
549 by a longer term climate and surrounding environments. Considering that the surface water
550 source is mainly from snow melt in the upper Boise River Basin, the available water of an irrigation
551 season in the study area is strongly affected by the precipitation from the current spring and the
552 previous winter in the upper watershed. As such, the annual summation of the allocated water is
553 a complex nonlinear issue as shown in Figure 9. For example, 2007 is a dry year, but the allocated
554 water is still relatively high due to the high precipitation rate in 2006 which releases abundant
555 snow melting from the upper watershed during the earlier irrigation season of 2007.

556 Nonetheless, Boise River has never been totally drained out in a single day during the simulation
557 period, and has abundant water to be diverted. More accurate discharge matching the historical
558 record is not a deciding factor for irrigation activities in the area, and the downstream water
559 balance mismatch is currently not an influencing factor for irrigation distribution.



560 Despite the limitations and challenges, the results generated by this research have successfully
561 integrated irrigation activities into a hydrological model and can serve as a good start for further
562 studies. The current study also proves that the integrated modeling work can provide sufficient
563 spatial and temporal details to nevertheless provide useful insights into possible management
564 strategies for water use in the Treasure Valley.

565 4.3 Insights and future work

566 This work is built under a larger on-going modeling framework that aims to integrate complex
567 social and biophysical processes and reveals the requirement of multi-disciplinary corporation.
568 Our experience suggests that deploying such an interdisciplinary approach is by no means a
569 trivial task. During our research, a large team of scientists, engineers and stakeholders
570 continuously discuss and construct an agreement on the study domain which reflects both the
571 watershed boundary and political boundary, the research questions, the temporal scales and
572 the complexity of the work. Knowledge from local stakeholders are also borrowed to help justify
573 the design of the model. This research effort is an important step forward towards the solution to
574 the cultural and historical barrier to the integration across disciplines [Hamilton *et al.*, 2015].
575 As the first report of the modeling fruit, in this paper, we are using historical downscaled climate
576 data here to represent the climate, and the parameter set is only suitable for this specific case.
577 For the future research of water availability projection, a suite of different climate change
578 scenarios will be incorporated. Future modeling of this method will highlight changes in water
579 deficits over time by dynamically simulating IDU water demand and water availability. Water
580 rights are also going to be dynamically allocated with adoptive strategies when water scarcity is
581 more severe. In addition, other important factors such as urban growth, land use and land cover
582 change, and crop choice will also be integrated into the future model with the feedback of
583 stakeholders.

584 5. Conclusion

585 This study integrates spatially and temporally explicit irrigation activities into hydrologic cycles,
586 connecting agriculture, water rights and hydrologic processes in the semi-arid Treasure Valley.
587 The model results reveal the spatial and temporal patterns of irrigation water use, and areas
588 where current water rights are not always able to support irrigation demand. The model is useful
589 in that it can be used to diagnose places of use and times where allocated water is likely
590 insufficient to meet agricultural water demands, and inform future water management decisions.



591 The modeling framework is extensible and allows not only for the model to be subjected to future
592 scenarios of urbanization and climate change, but also as a tool for evaluating alternative future
593 scenarios of water management policies and actions. The model also indicates the current
594 knowledge gap in water use between the water rights based diversion rate and the actual irrigation
595 water consumption, including the complexity of human activities and the inability to fully capture
596 the discharge over dry years.

597 **Author contributions:** Bangshuai Han and Alejandro N. Flores designed this research and interpreted
598 the results. John Bolte and Kellie B. Vache provided technical support with debugging help. Bangshuai Han
599 prepared the manuscript with the help with Shawn Benner, Alejandro N. Flores, and get agreement for
600 submission with all co-authors.

601 **ACKNOWLEDGMENTS**

602 This publication was made possible by the NSF Idaho EPSCoR Program and by the National
603 Science Foundation under award number IIA-1301792. We appreciate James Sulzman and
604 Cynthia Schwartz for the help during the modeling processes.

605 **REFERENCES**

- 606 Abatzoglou, J. T., and T. J. Brown (2012), A comparison of statistical downscaling methods suited for
607 wildfire applications, *International Journal of Climatology*, 32(5), 772-780.
- 608 Abebe, N. A., F. L. Ogden, and N. R. Pradhan (2010), Sensitivity and uncertainty analysis of the conceptual
609 HBV rainfall–runoff model: Implications for parameter estimation, *Journal of hydrology*, 389(3), 301-310.
- 610 Ahrends, H., M. Mast, C. Rodgers, and H. Kunstmann (2008), Coupled hydrological–economic modelling
611 for optimised irrigated cultivation in a semi-arid catchment of West Africa, *Environmental Modelling &*
612 *Software*, 23(4), 385-395.
- 613 Allen, R. G., and C. W. Robison (2007), Evapotranspiration and consumptive irrigation water requirements
614 for Idaho, *Precipitation Deficit Table for Boise WSFO Airport*.
- 615 Barros, A., A. Ager, H. Preisler, M. Day, T. Spies, and J. Bolte (2015), Understanding coupled natural and
616 human systems on fire prone landscapes: integrating wildfire simulation into an agent based planning
617 system, paper presented at *EGU General Assembly Conference Abstracts*, Vienna, Austria, 2015.
- 618 Bolte, J., and K. Vache (2010), Envisioning Puget Sound Alternative Futures, *Oregon State University*.
- 619 Bolte, J. P., D. W. Hulse, S. V. Gregory, and C. Smith (2007), Modeling biocomplexity–actors, landscapes
620 and alternative futures, *Environmental Modelling & Software*, 22(5), 570-579.
- 621 Cai, W. J., L. L. Zhang, X. P. Zhu, A. J. Zhang, J. X. Yin, and H. Wang (2013), Optimized reservoir operation
622 to balance human and environmental requirements: A case study for the Three Gorges and Gezhouba
623 Dams, Yangtze River basin, China, *Ecological Informatics*, 18, 40-48.
- 624 Cai, X., Y. Cui, J. Dai, and Y. Luo (2012), Local storages: the impact on hydrology and implications for
625 policy making in irrigation systems, *Water International*, 37(4), 395-407.
- 626 Collins, S. L., et al. (2011), An integrated conceptual framework for long-term social–ecological research,
627 *Frontiers in Ecology and the Environment*, 9(6), 351-357.
- 628 Dam, v. J. C., J. Huygen, J. G. Wesseling, R. A. Feddes, P. Kabat, v. P. E. V. Walsum, P. Groenendijk, and
629 v. C. A. Diepen (1997), Theory of SWAP version 2.0; Simulation of water flow, solute transport and plant
630 growth in the Soil-Water-Atmosphere-Plant environment.



- 631 Di Baldassarre, G., M. Kooy, J. S. Kemerink, and L. Brandimarte (2013), Towards understanding the
 632 dynamic behaviour of floodplains as human-water systems, *Hydrology and Earth System Sciences*, 17(8),
 633 3235-3244.
- 634 Donigian, A. S. (2002), Watershed model calibration and validation: The HSPF experience, *Proceedings of*
 635 *the Water Environment Federation*, 2002(8), 44-73.
- 636 Droogers, P., W. G. M. Bastiaanssen, M. Beyazgül, Y. Kayam, G. W. Kite, and H. Murray-Rust (2000),
 637 Distributed agro-hydrological modeling of an irrigation system in western Turkey, *Agricultural Water*
 638 *Management*, 43(2), 183-202.
- 639 Döll, P., and S. Siebert (2002), Global modeling of irrigation water requirements, *Water Resources*
 640 *Research*, 38(4), 8-1.
- 641 Falkenmark, M. (2013), Adapting to climate change: towards societal water security in dry-climate countries,
 642 *International Journal of Water Resources Development*, 29(2), 123-136.
- 643 Ferguson, I. M., and R. M. Maxwell (2012), Human impacts on terrestrial hydrology: climate change versus
 644 pumping and irrigation, *Environmental Research Letters*, 7(4), 044022.
- 645 Gassman, P. W., J. R. Williams, V. W. Benson, R. C. Izaurralde, L. M. Hauck, C. A. Jones, J. D. Atwood,
 646 J. R. Kiniry, and J. D. Flowers (2005), *Historical development and applications of the EPIC and APEX*
 647 *models*, Center for Agricultural and Rural Development, Iowa State University Ames.
- 648 Girard, C., J.-D. Rinaudo, M. Pulido-Velazquez, and Y. Caballero (2015), An interdisciplinary modelling
 649 framework for selecting adaptation measures at the river basin scale in a global change scenario,
 650 *Environmental Modelling & Software*, 69, 42-54.
- 651 Gisser, M., and A. Mercado (1972), Integration of the agricultural demand function for water and the
 652 hydrologic model of the Pecos basin, *Water Resources Research*, 8(6), 1373-1384.
- 653 Gupta, H. V., S. Sorooshian, and P. O. Yapo (1998), Toward improved calibration of hydrologic models:
 654 Multiple and noncommensurable measures of information, *Water Resources Research*, 34(4), 751-763.
- 655 Hamilton, S. H., S. ElSawah, J. H. A. Guillaume, A. J. Jakeman, and S. A. Pierce (2015), Integrated
 656 assessment and modelling: overview and synthesis of salient dimensions, *Environmental Modelling &*
 657 *Software*, 64, 215-229.
- 658 Hutchins, W. A. (1977), *Water Rights Laws in the Nineteen Western States*, Natural Resource Economics
 659 Division, Economic Research Service, United States Department of Agriculture.
- 660 Huter, L.R., R.L. Mahler, L.E. Brooks, B.A. Lolley, and L. Halloway (1999). Groundwater and wellhead
 661 protection in the HUA. *UI Bull. 811*. Univ. of Idaho, Moscow.
- 662 Inouye, A. M. (2014), Development of a hydrologic model to explore impacts of climate change on water
 663 resources in the Big Wood Basin, Idaho.
- 664 Jakeman, A. J., and R. A. Letcher (2003), Integrated assessment and modelling: features, principles and
 665 examples for catchment management, *Environmental Modelling & Software*, 18(6), 491-501.
- 666 Kirby, J. M., M. Mainuddin, M. D. Ahmad, and L. Gao (2013), Simplified monthly hydrology and irrigation
 667 water use model to explore sustainable water management options in the Murray-Darling Basin, *Water*
 668 *resources management*, 27(11), 4083-4097.
- 669 Laniak, G. F., G. Olchin, J. Goodall, A. Voinov, M. Hill, P. Glynn, G. Whelan, G. Geller, N. Quinn, and M.
 670 Blind (2013), Integrated environmental modeling: a vision and roadmap for the future, *Environmental*
 671 *Modelling & Software*, 39, 3-23.
- 672 Lawrence, D., I. Haddeland, and E. Langsholt (2009), Calibration of HBV hydrological models using PEST
 673 parameter estimation, *Oslo, Norway: Norwegian Water Resources and Energy Directorate*.
- 674 Legesse, D., C. Vallet-Coulomb, and F. Gasse (2003), Hydrological response of a catchment to climate
 675 and land use changes in Tropical Africa: case study South Central Ethiopia, *Journal of Hydrology*, 275(1),
 676 67-85.
- 677 Leng, G., M. Huang, Q. Tang, H. Gao, and L. R. Leung (2014), Modeling the effects of groundwater-fed
 678 irrigation on terrestrial hydrology over the conterminous United States, *Journal of Hydrometeorology*, 15(3),
 679 957-972.
- 680 Liu, J., J. R. Williams, A. J. B. Zehnder, and H. Yang (2007), GEPIC—modelling wheat yield and crop water
 681 productivity with high resolution on a global scale, *Agricultural Systems*, 94(2), 478-493.
- 682 Montes de Oca Munguia, O., G. Harmsworth, R. Young, and J. Dymond The use of an agent-based model
 683 to represent Māori cultural values, 2009.
- 684 Neibling, H. (1997), *Irrigation systems for Idaho agriculture*, University of Idaho, College of Agriculture,
 685 Cooperative Extension System, Agricultural Experiment Station.



- 686 Pahl-Wostl, C. (2007), Transitions towards adaptive management of water facing climate and gl, *Water*
687 *Resources Management*, 21(1), 49-62.
- 688 Petrich, C. R. (2004a), *Simulation of ground water flow in the lower Boise River Basin*, Idaho Water
689 Resources Research Institute.
- 690 Petrich, C. R. (2004b), *Treasure Valley hydrologic project executive summary*, Idaho Water Resources
691 Research Institute.
- 692 Ryan, J. G., and D. C. Spencer (2001), *Future challenges and opportunities for agricultural R&D in the*
693 *semi-arid tropics*, International Crops Research Institute for the Semi-Arid Tropics.
- 694 Shiklomanov, I. A. (2000), Appraisal and assessment of world water resources, *Water international*, 25(1),
695 11-32.
- 696 Sorooshian, S., J. Li, K. I. Hsu, and X. Gao (2012), Influence of irrigation schemes used in regional climate
697 models on evapotranspiration estimation: Results and comparative studies from California's Central Valley
698 agricultural regions, *Journal of Geophysical Research: Atmospheres (1984–2012)*, 117(D6).
- 699 Stöckle, C. O., M. Donatelli, and R. Nelson (2003), CropSyst, a cropping systems simulation model,
700 *European journal of agronomy*, 18(3), 289-307.
- 701 Stöckle, C. O., A. R. Kemanian, R. L. Nelson, J. C. Adam, R. Sommer, and B. Carlson (2014), CropSyst
702 model evolution: from field to regional to global scales and from research to decision support systems,
703 *Environmental Modelling & Software*, 62, 361-369.
- 704 Sælthun, N. R. (1996), The Nordic HBV model, *Norwegian Water Resources and Energy Administration*
705 *Publication*, 7, 1-26.
- 706 Terrado, M., V. Acuna, D. Ennaanay, H. Tallis, and S. Sabater (2014), Impact of climate extremes on
707 hydrological ecosystem services in a heavily humanized Mediterranean basin, *Ecological Indicators*, 37,
708 199-209.
- 709 Turner, D. P., D. R. Conklin, and J. P. Bolte (2015), Projected climate change impacts on forest land cover
710 and land use over the Willamette River Basin, Oregon, USA, *Climatic Change*, 1-14.
- 711 Urban, S. M., and C. R. Petrich (1996), water budget for the Treasure Valley aquifer system, *Treasure*
712 *Valley Hydrologic Project Research Report*, Idaho Department of Water Resources, Boise, Idaho.
- 713 Vörösmarty, C. J., P. Green, J. Salisbury, and R. B. Lammers (2000), Global Water Resources: Vulnerability
714 from Climate Change and Population Growth.
- 715 Willaarts, B. A., M. Volk, and P. A. Aguilera (2012), Assessing the ecosystem services supplied by
716 freshwater flows in Mediterranean agroecosystems, *Agricultural Water Management*, 105, 21-31.
- 717 Wurbs, R. A. (2005a), Texas water availability modeling system, *Journal of Water Resources Planning and*
718 *Management*, 131(4), 270-279.
- 719 Wurbs, R. A. (2005b), Modeling river/reservoir system management, water allocation, and supply reliability,
720 *Journal of Hydrology*, 300(1), 100-113.
- 721 Xu, W., S. E. Lowe, and R. M. Adams (2014), Climate change, water rights, and water supply: The case of
722 irrigated agriculture in Idaho, *Water Resources Research*.
- 723 <https://www.idwr.idaho.gov/WaterInformation/Projects/tvhp-revised/>
724



725

Table 1 Datasets used in the model

Input Data	Data Sources	Dates	Used in Model Components	Url
Land use/land cover	National Landcover dataset (NLCD)	2011	Evapotranspiration	http://www.mrlc.gov/nlcd2011.php
Streams/canals /Water bodies	NHDPlus V2	2012	Building stream network and flow routing	http://www.horizon-systems.com/nhdplus/NHDPlusV2_17.php
Downscaled climate data	U of Idaho METDATA (4 km resolution)	2006-2013	Evapotranspiration	http://cida.usgs.gov/thredds/catalog.html?dataset=cida.usgs.gov/thredds/UofIMETDATA
Daily stream discharge	USGS Instantaneous Data Archive	2006-2013	Hydrology model calibration and validation	http://nwis.waterdata.usgs.gov/nwis/rt
Digital elevation model	NED (30 m resolution)	N/A	Building HRU	http://nationalmap.gov/elevation.html
Water rights	Idaho Department of Water Resources	2010	Irrigation (Watermaster)	http://www.idwr.idaho.gov/ftp/gisdata/Spatial/WaterRights

726
 727



728 Table 2 Crop categories used to approximate the land use categories in the ET calculation

Land use category	Approximated Crops in ET calculation
Agricultural	Alfalfa
Developed land	Bare land
Forest	Poplar
Shrubland	Sagebrush
Herbaceous	Average of Cheatgrass, bunch grass and brome grass

729



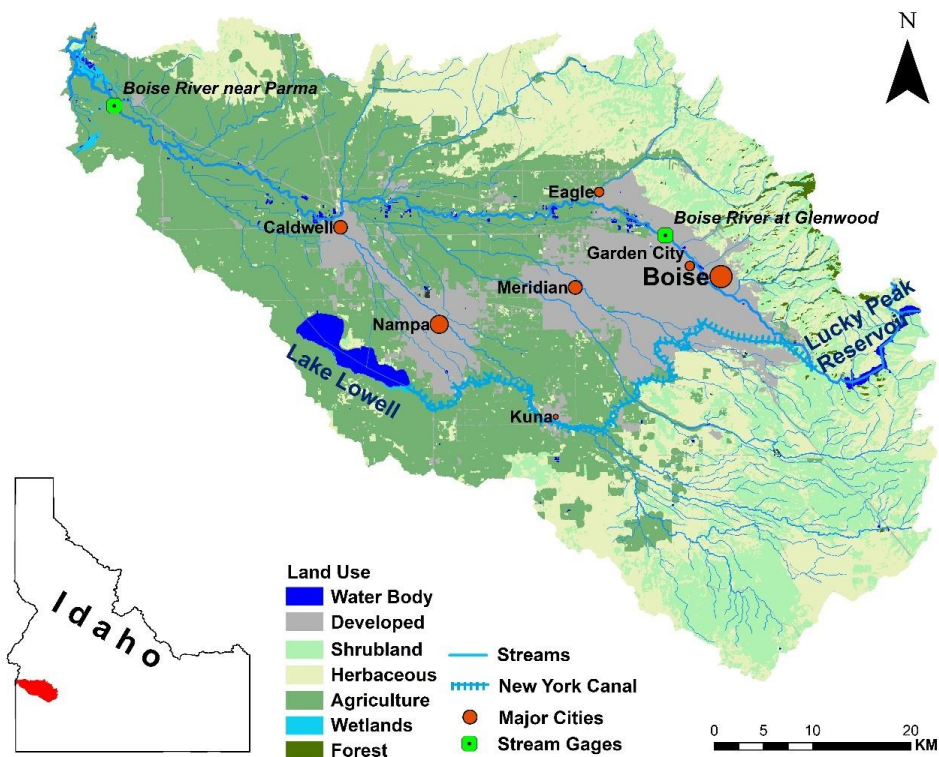
730 Table 3 Parameters used, the range considered for calibration and the calibrated values

Routine	Parameter	Description	Units	Range Considered	Calibrated Value
Snow Routine	TT	Threshold temperature	°C	-2.0 - 2.0	0.4
	CFMAX	Degree-day factor governing maximum snowmelt rate	mm/°C /day	1.0 - 6.0	3.6
	SFCF	Snowmelt correction factor	-	0.5 - 3.0	2.2
	CFR	Refreeze coefficient	-	0.05	0.05
	CWH	Water holding capacity of snowpack	-	0.1	0.1
Soil and Evaporation Routine	FC	Maximum depth of water in soil water reservoir	mm	395	395
	LP	Soil moisture value above which actual ET = PET	mm	200.0	200
	WP	Wilting point in soil for ET to occur	mm	147	147
	BETA	Shaping Coefficient	-	1.0 - 6.0	2.6
Ground-water and Response Routine	PERC	Percolation coefficient	per day	0.1 - 10.0	6.6
	UZL	Threshold for K0 to outflow	mm	10.0 - 500.0	240.7
	K0	Recession coefficient	per day	0.1 - 1	0.7
	K1	Recession coefficient	per day	0.01 - 1.0	0.07
	K2	Recession coefficient	per day	0.0001 - 1.0	0.0002

731
 732
 733
 734
 735
 736



737



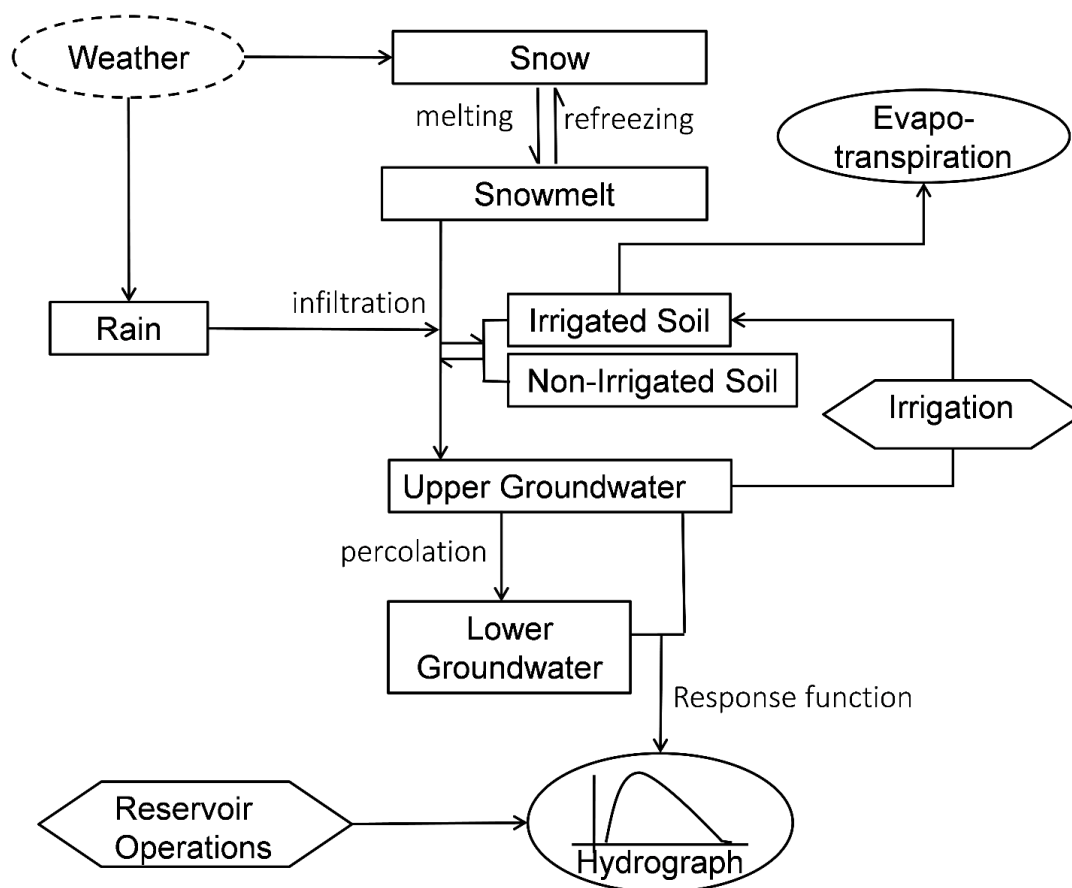
738

739 Figure 1 Study Area: The Treasure Valley which is located at Southwest Idaho, with Idaho's
740 three largest cities and complex agricultural activities.

741



742



743

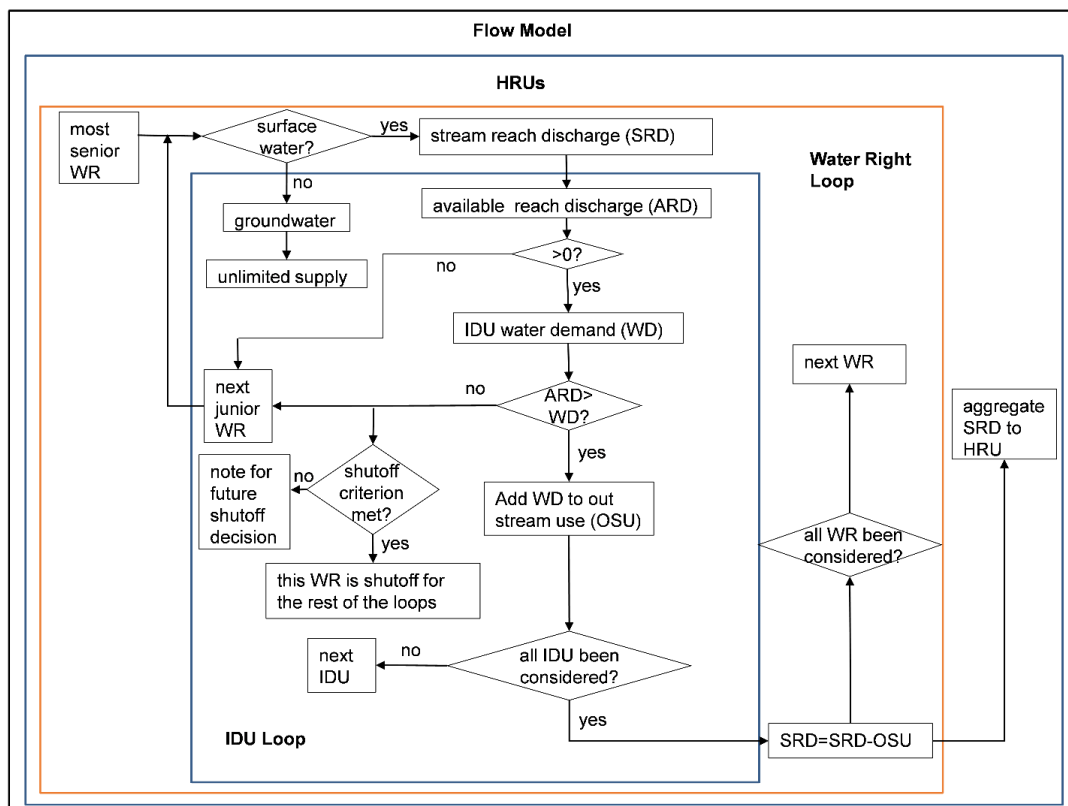
744

745

746

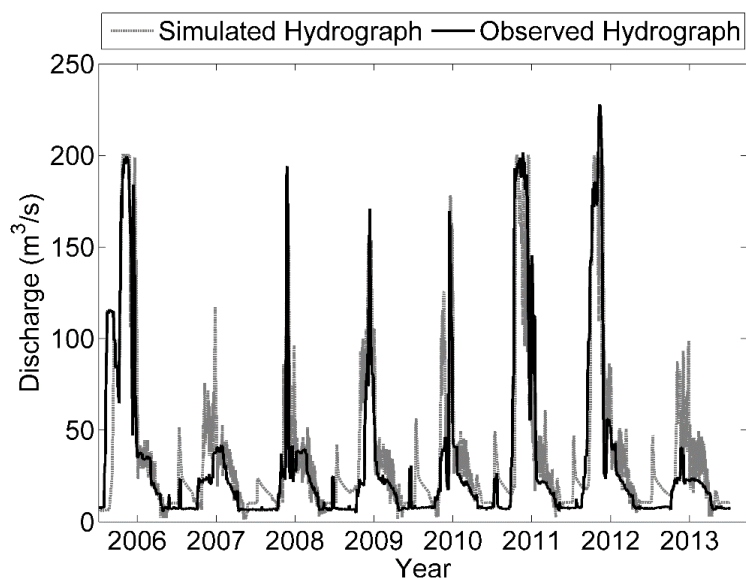
Figure 2 Flowchart of the Flow model in Envision. Note the human activities influencing water availability. Water is distributed by the local water rights data (irrigation activities), and is also constrained by the reservoir operations.

747

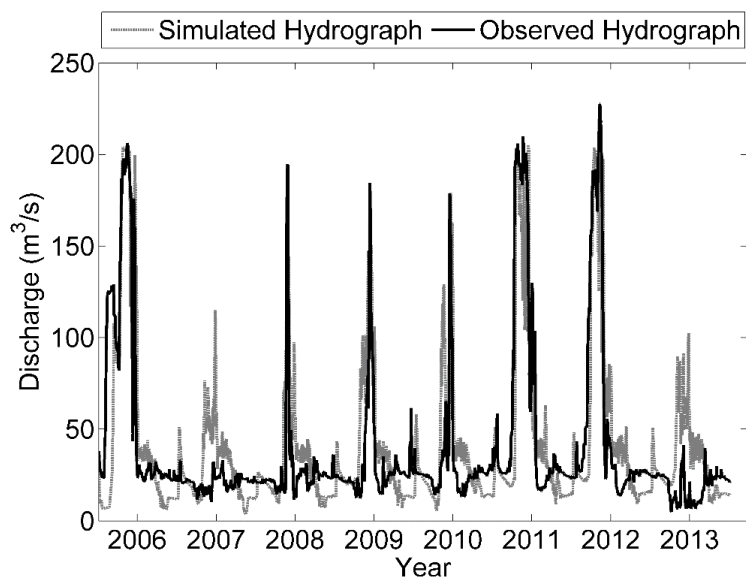


748
 749
 750
 751
 752

Figure 3 Flowchart of the water right loop in Envision. Each water right is first appropriated for each IDU it applies to. At each flow time step, the stream reach discharge is then aggregated to the HRU level, and used for the next time step.



753



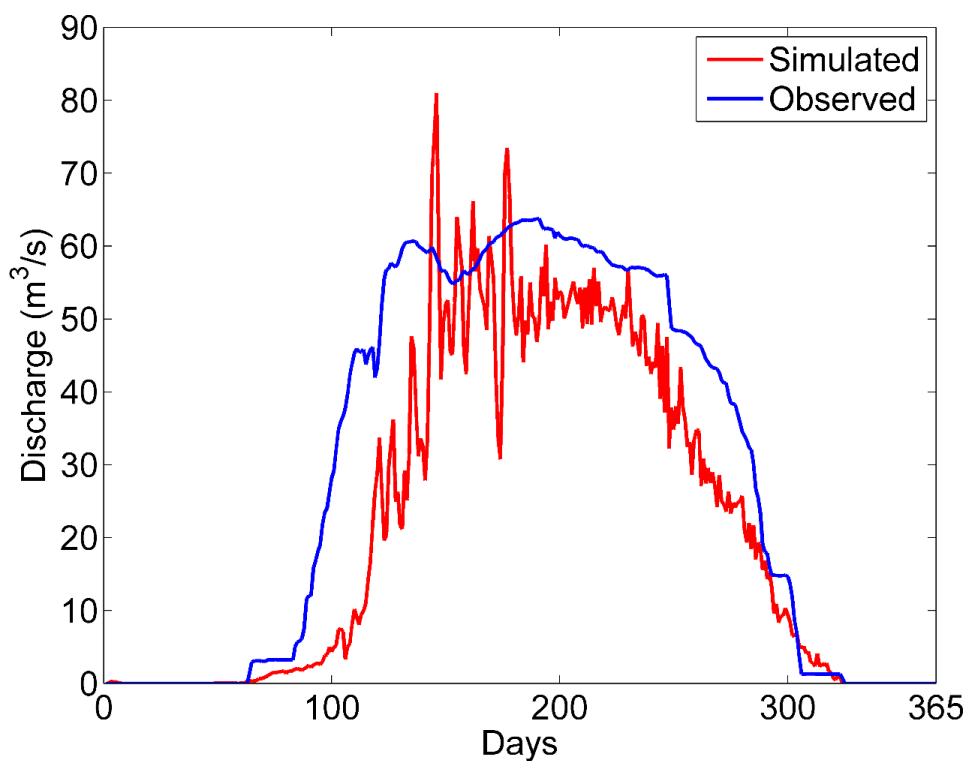
754

755

756 Figure 4 Simulated discharge and the observations during the calibration (2006 ~ 2009) and
757 validation periods (2010 ~ 2013) at the Glenwood Station of Boise River (Upper Panel) and
758 Parma Station of Boise River (Lower Panel).



759

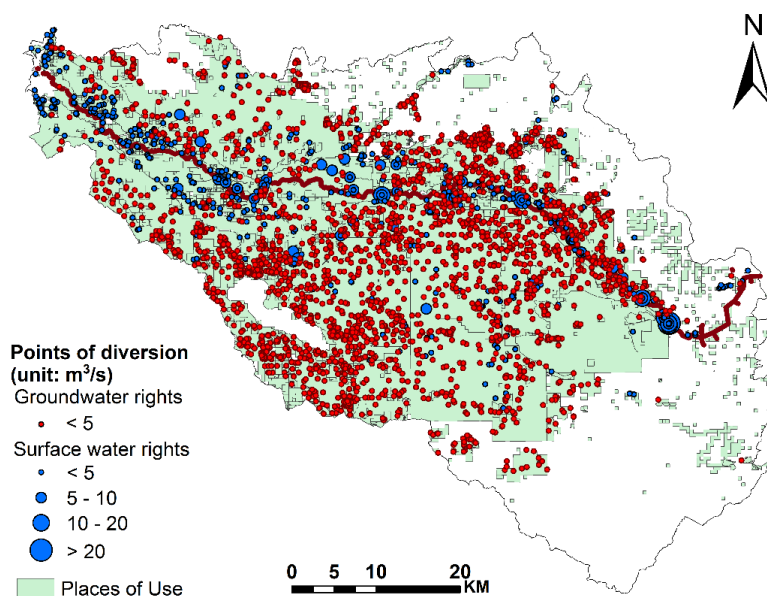


760

761 Figure 5 Simulated irrigation amount and the observations averaged over the years of 2006 ~
762 2013 at the New York Canal. Blue color lines are daily discharge rate in m^3/s , and red color
763 lines are cumulative discharge in m^3 .

764

765

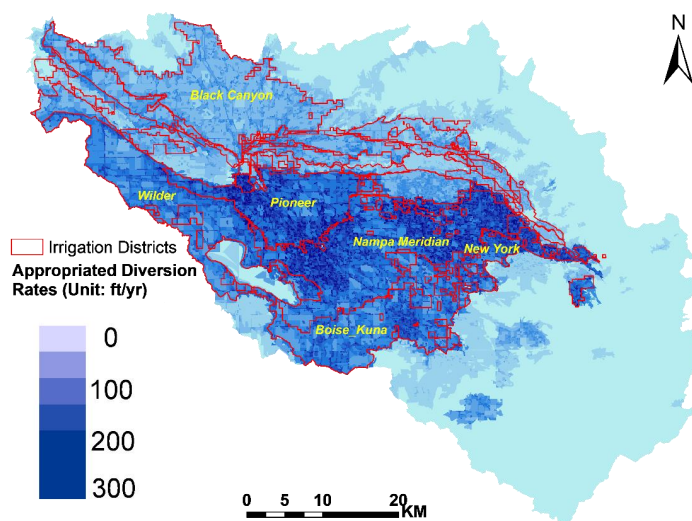


766
767
768
769
770
771

Figure 6 The maximum allowed diversion rates and the spatial distribution of the Points of Diversion (PODs). Note that multiple diversion PODs overlap at the New York Canal diversion places, and the water diverted from New York Canal serves as the main surface water resources for the agricultural areas.

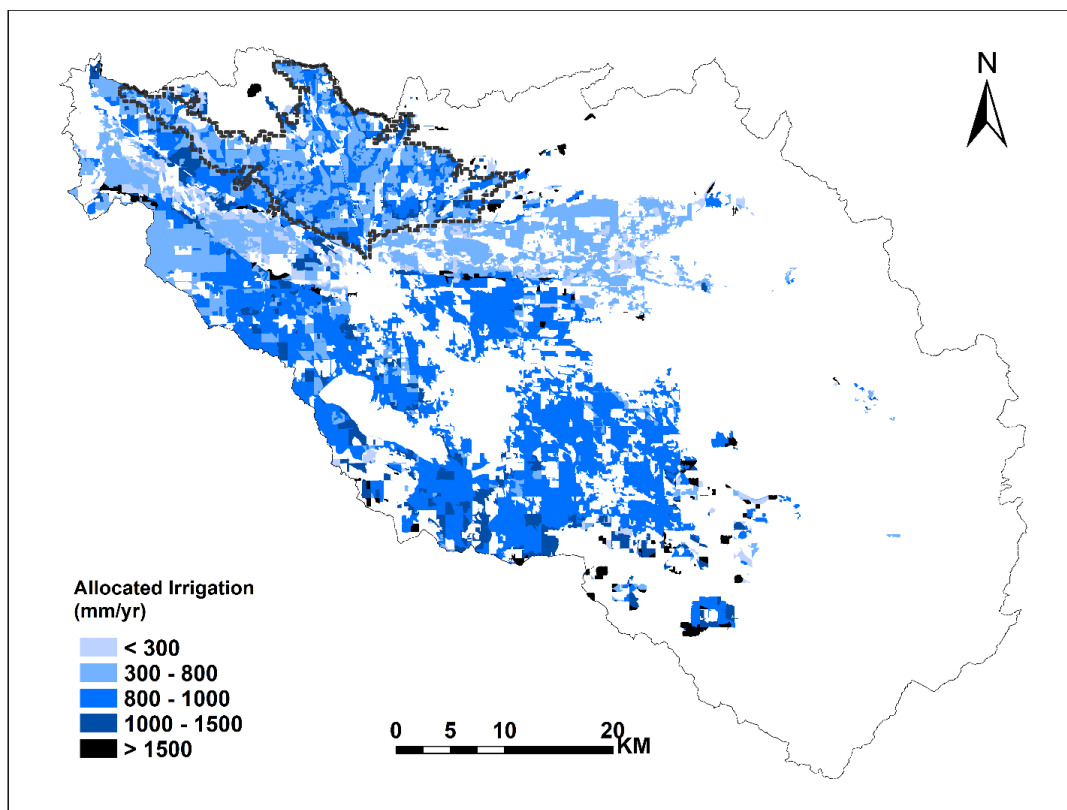


772



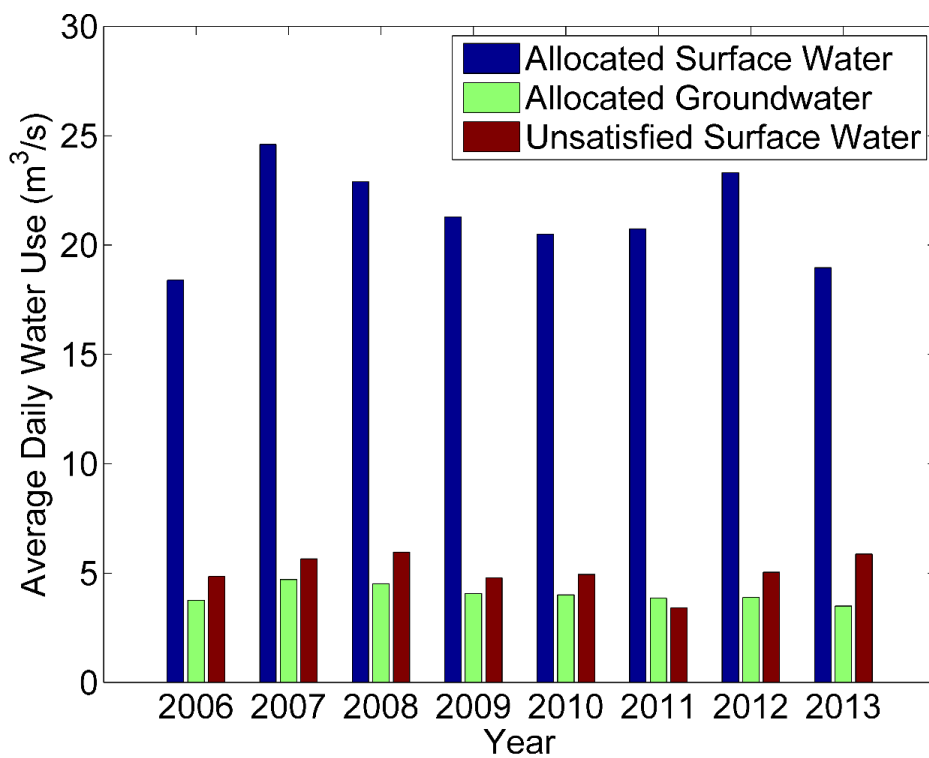
773
774
775
776
777
778
779

Figure 7 The annual appropriated diversion rates calculated based on water rights maximum allowed diversion rates and place of use, indicating the potential usable water. The irrigation district boundaries and the names of major irrigation districts are also shown.



780
781
782
783
784
785
786

Figure 8 The spatial distribution of the annual allocated irrigation water averaged over the simulation period. The domain that is within the dotted circle is Black Canyon Irrigation District, which receives additional irrigation water from outside of the domain, where the water allocation is underestimated.

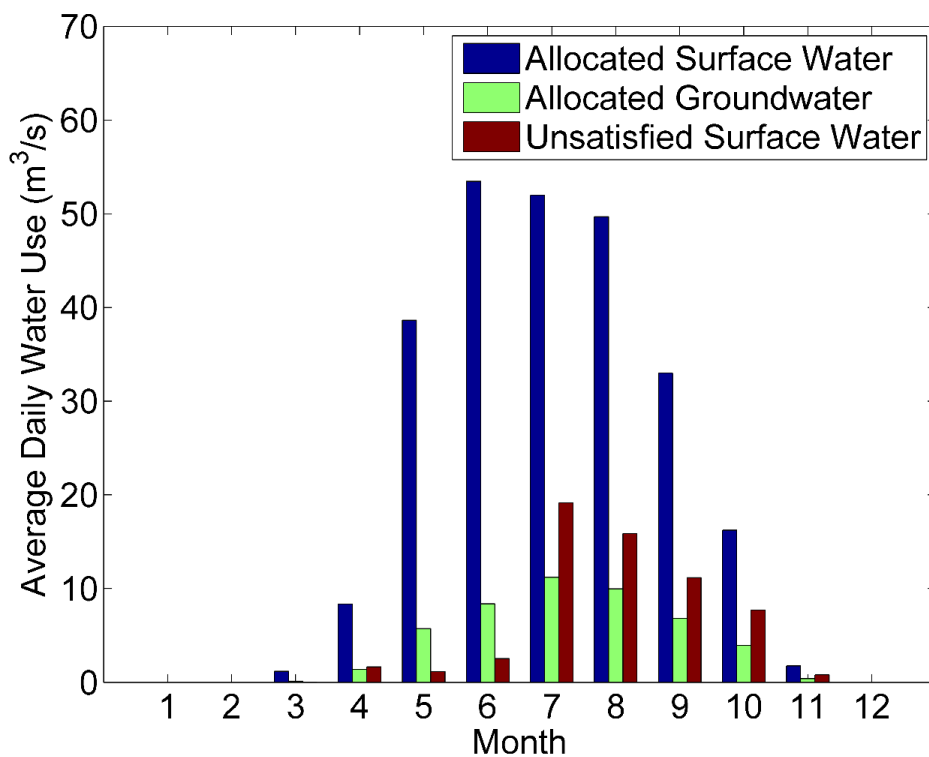


787
788
789
790

Figure 9: Average daily allocated surface water, groundwater and unsatisfied surface water use for each year.

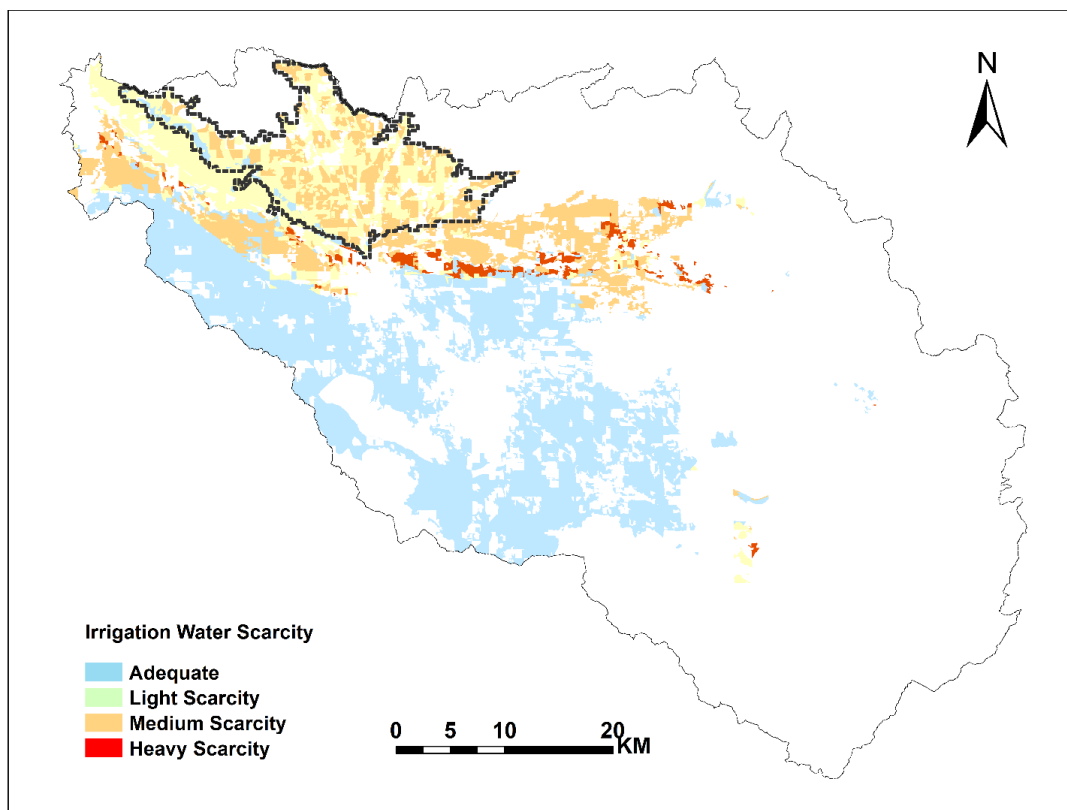


791
792
793



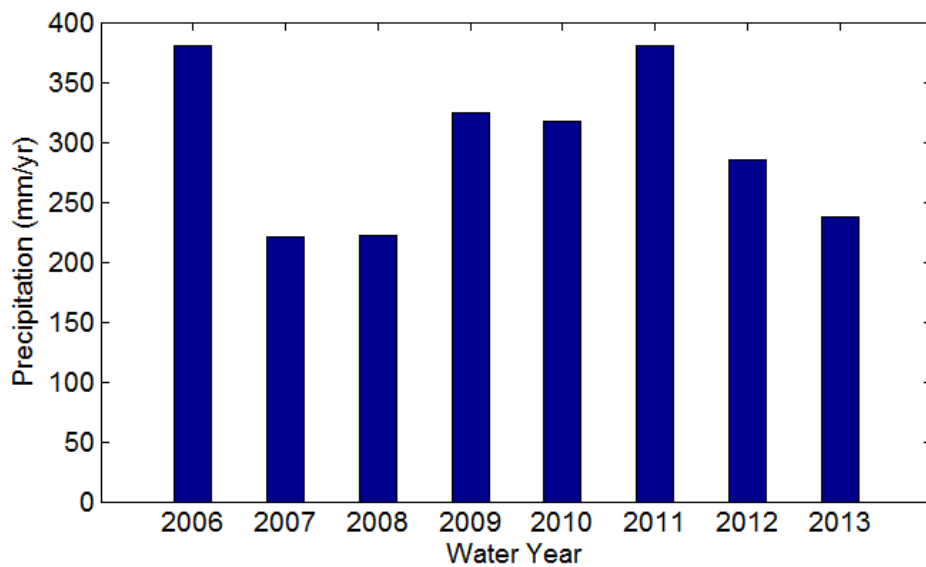
794
795
796
797
798

Figure 10: Average daily allocated surface water, groundwater and unsatisfied surface water use for each month from 2006 to 2013.



799
800
801
802
803
804
805
806

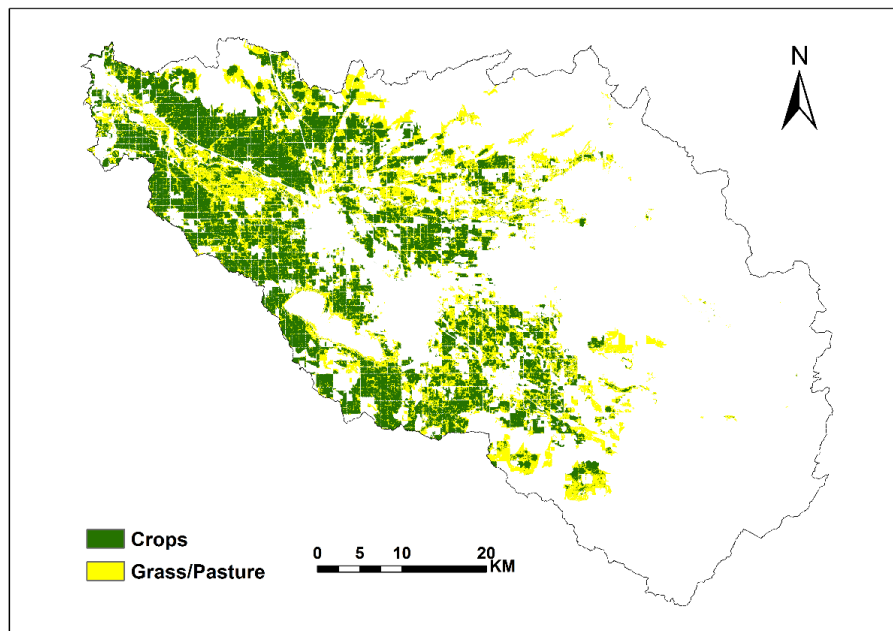
Figure 11: The spatial distribution of the annual unsatisfied irrigation maps averaged over the simulation period. The domain that is circled is Black Canyon Irrigation District, which receives additional irrigation water from outside of the domain, where the water scarcity is overestimated.



807
808
809
810

811
812

Figure 12 Annual precipitation amount calculated at Boise Air Terminal (Station ID: 7268104131). Precipitation is calculated based on water year since irrigation in each calendar year is mainly affected by the precipitation during the spring and last winter.



813

814

815

816

Figure 13 The spatial distribution of crops and grass/pasture in the agricultural area of the Treasure Valley.